Electronic Supplementary Material (ESI) for Journal of Materials Chemistry A.

Supporting Information for "Interfacial Dynamics of Carbon Interlayers in Anode-free Solid-State Batteries"

Daniel W. Liao[1], Tae H. Cho[1], Shaurya Sarna[1], Manoj K. Jangid[1], Hiroki Kawakam[2], Toshikazu Kotaka[2], Koichiro Aotani[2], Neil P. Dasgupta[1,3,]*

1 Department of Mechanical Engineering, University of Michigan, Ann Arbor, MI, 48109 USA
2 Nissan Research Center, Nissan Motor Co., Ltd., Natsushima, Yokosuka, Kanagawa 237-8523, Japan
3 Department of Materials Science and Engineering, University of Michigan, Ann Arbor, MI, 48109 USA
** Corresponding Author. E-mail Address: ndasgupt@umich.edu*

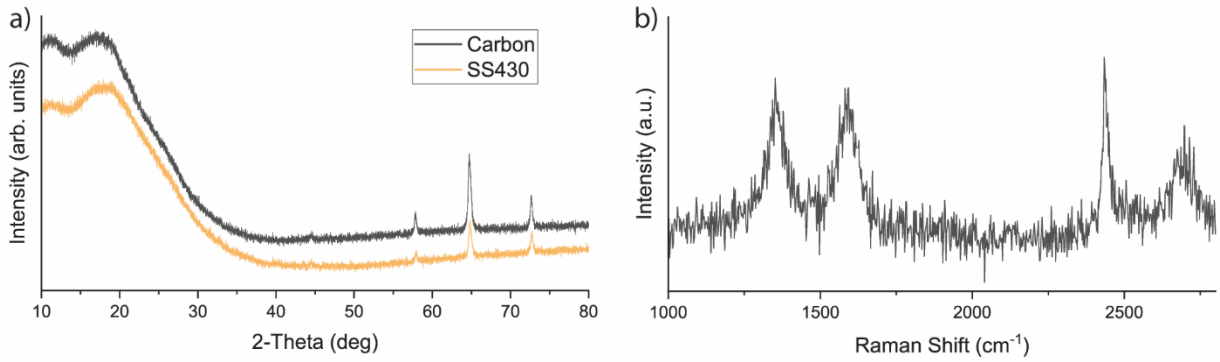

Figure S1. XRD and Raman spectroscopy of carbon interlayer. a) XRD and b) Raman spectroscopy performed on a carbon surface as deposited on SS430 foil

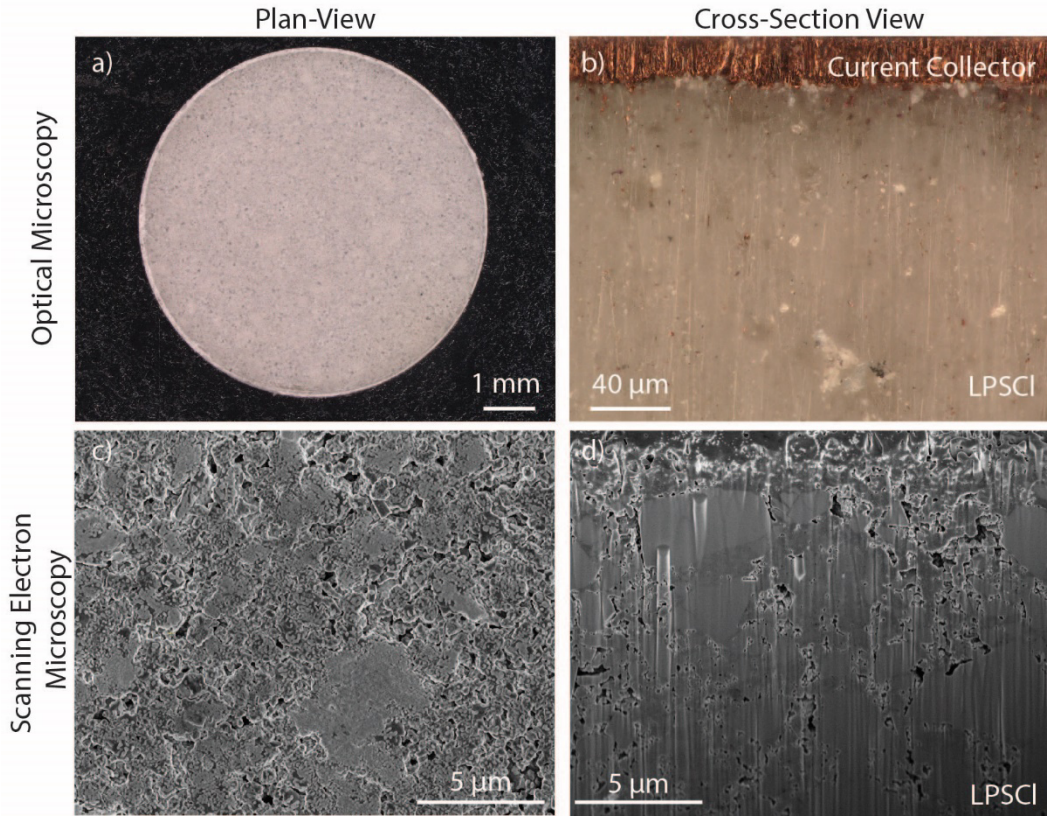

Figure S2. Optical and scanning electron microscopy of LPSCl pellet. Optical microscopy (a) plane-view and (b) cross-section of carbon and SEM image (c) plane-view and (d) Plasma focused-ion beam (PFIB) cross-section of carbon interlayer on LPSCl solid electrolyte pellet. (e) Resulting Cu/LPSCl/Li cell configuration

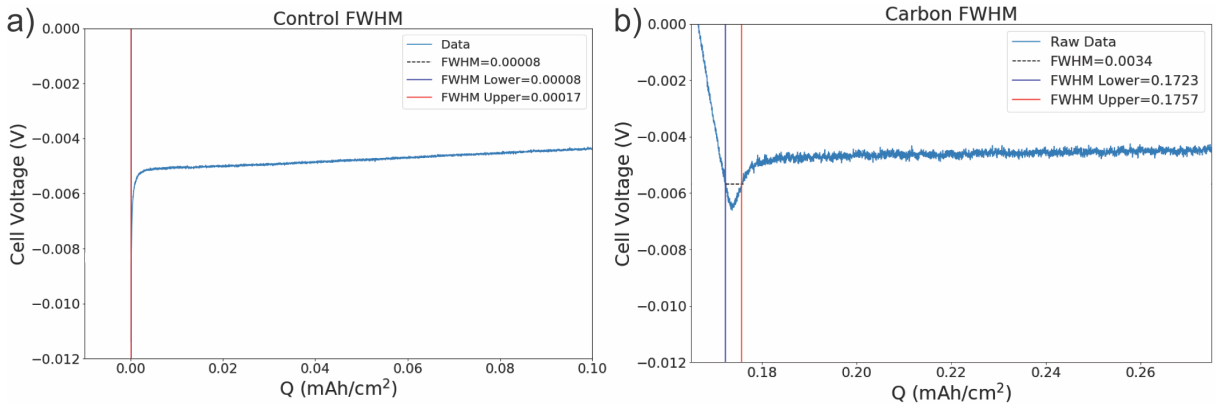

Figure S3. Full width half maximum (FWHM)of nucleation peak. Galvanostatic charging at 0.1 mA/cm^2 with measured FWHM for (a) control and (b) carbon interlayer sample.

Table 1: Minimum nucleation potential for sample with and without carbon interlayer during charging at various current densities

Current Density mA/cm^2	Control	Carbon
	Nucleation Potential (mV)	Nucleation Potential (mV)
0.01	-5.47	-3.70
0.1	-14.74	-6.61
0.2	-16.35	-8.54
0.5	-22.26	-12.83
1.0	-26.94	-22.40

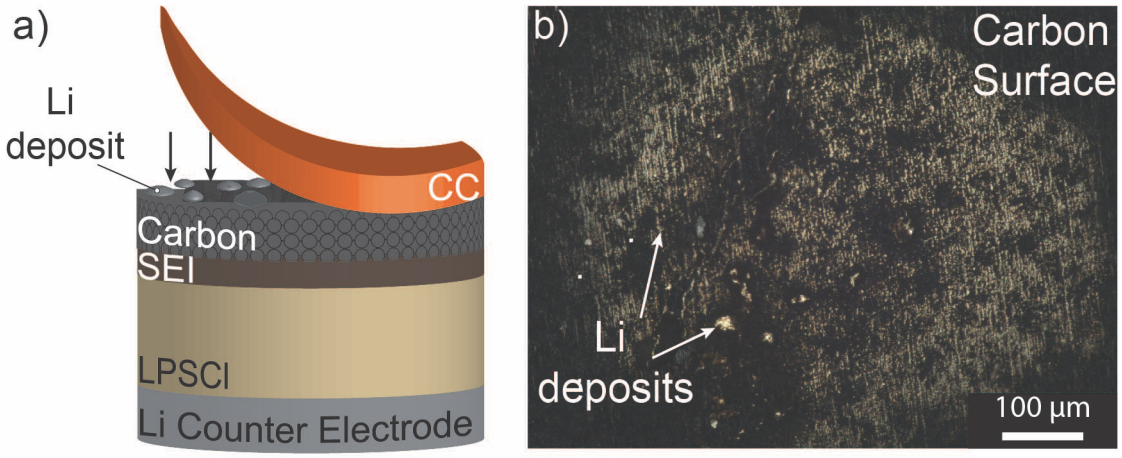

Figure S4. Optical Microscopy of carbon surface after Li plating. (a) Schematic of sample with carbon interlayer Cu/Carbon-LPSCl/Li for post-mortem optical imaging. (b) Plan-view image of carbon surface after deposition of 0.3 mAh/cm^2 at a current density of 0.1 mA/cm^2.

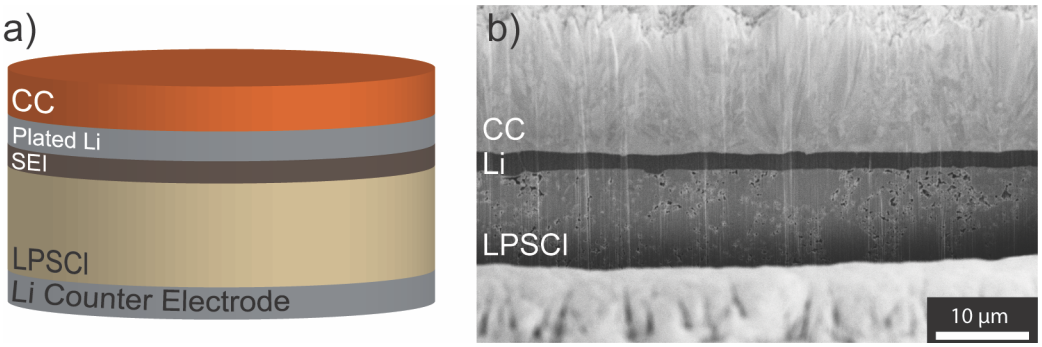

Figure S5. Plated Li for a control sample. (a) Schematic of control sample without carbon Cu/LPSCl/Li. (b) PFIB cross-section after galvanostatic charging of at 0.1 mA/cm^2 for a capacity of 0.15 mAh/cm^2.

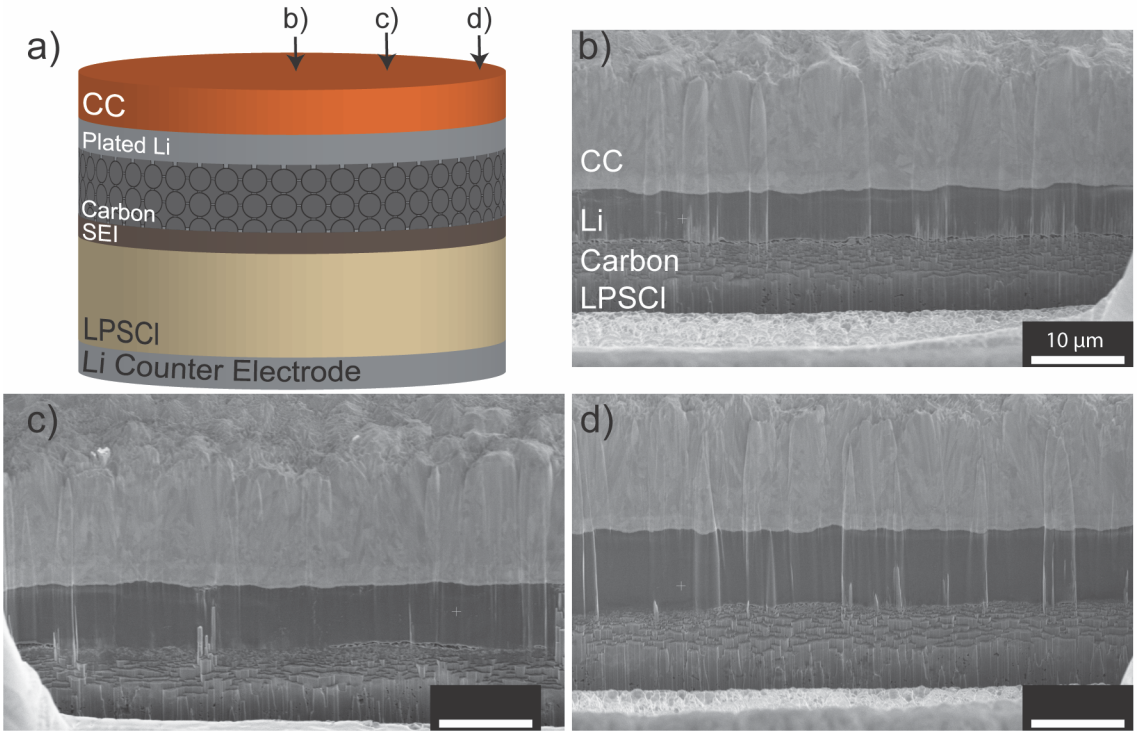

Figure S6. PFIB performed at different spatial locations. (a) Schematic of a sample with a carbon interlayer, showing the spatial locations of cross-sectional images across the sample. PFIB cross-sectional images at the (b) center, (c) middle, and (d) edge locations after galvanostatic charging at 0.1 mA/cm^2 for a capacity of 2.0 mAh/cm^2.

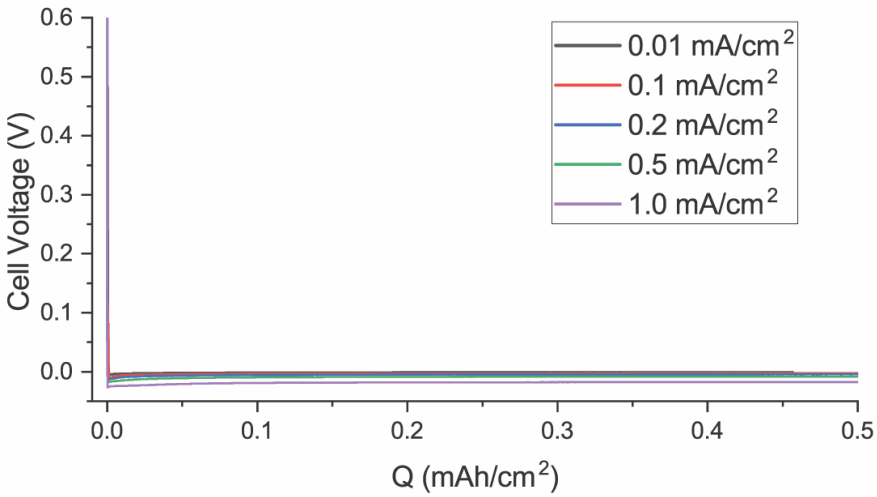

Figure S7 Charging of Cu/LPSCl/Li. First charge voltage profile of control samples without carbon during constant current charge at current densities of 0.01, 0.1, 0.2, 0.5, and 1.0 mA/cm^2.

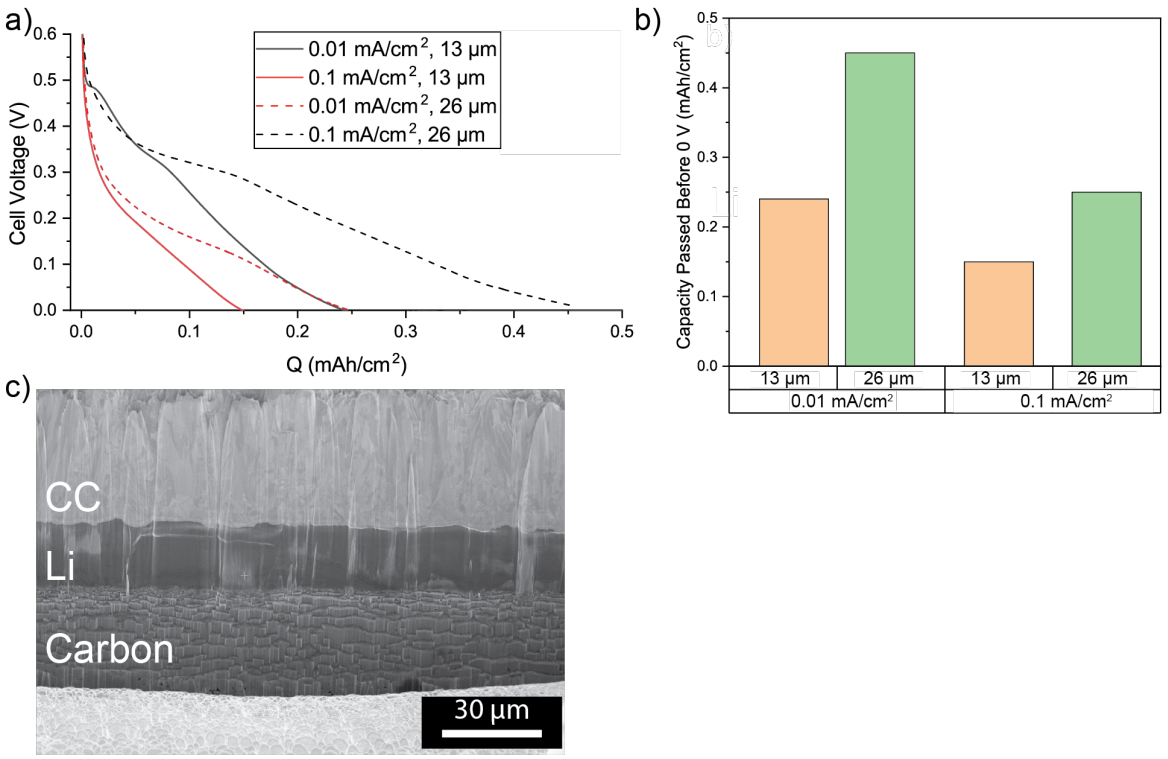

Figure S8. Effects of carbon interlayer thickness. (a) Voltage profiles during charging at a current density of 0.01 and 0.1 mA/cm^2, for different carbon interlayer thicknesses of 13 and 26 µm. (b) Cumulative capacity passed before reaching 0 V for each current density and carbon interlayer thickness. (c) Cross-sectional PFIB-SEM image of the 26 µm thick carbon interlayer after charging to a capacity of 2.0 mAh/cm^2.

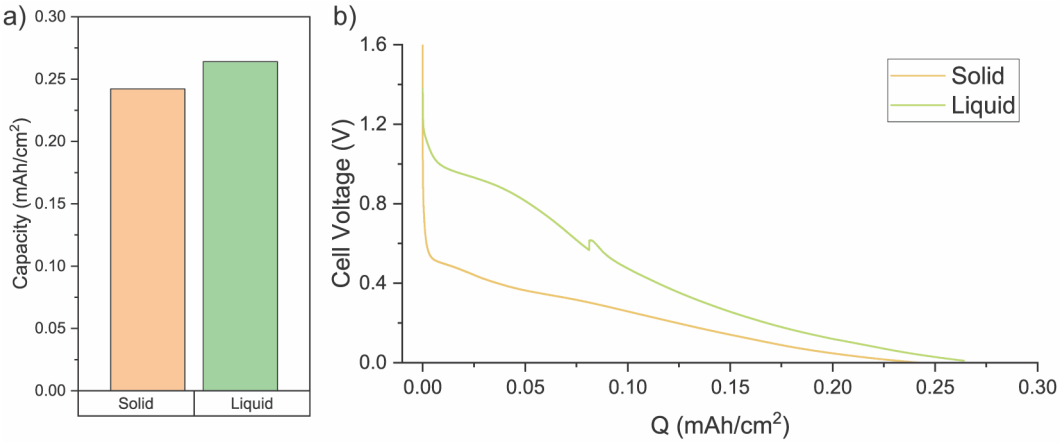

Figure S9. Capacity comparison with a liquid electrolyte system. (a) The total charge capacity and (b) the resulting voltage trace of the carbon interlayer using a solid electrolyte and liquid electrolyte to a cutoff voltage of 10 mV.

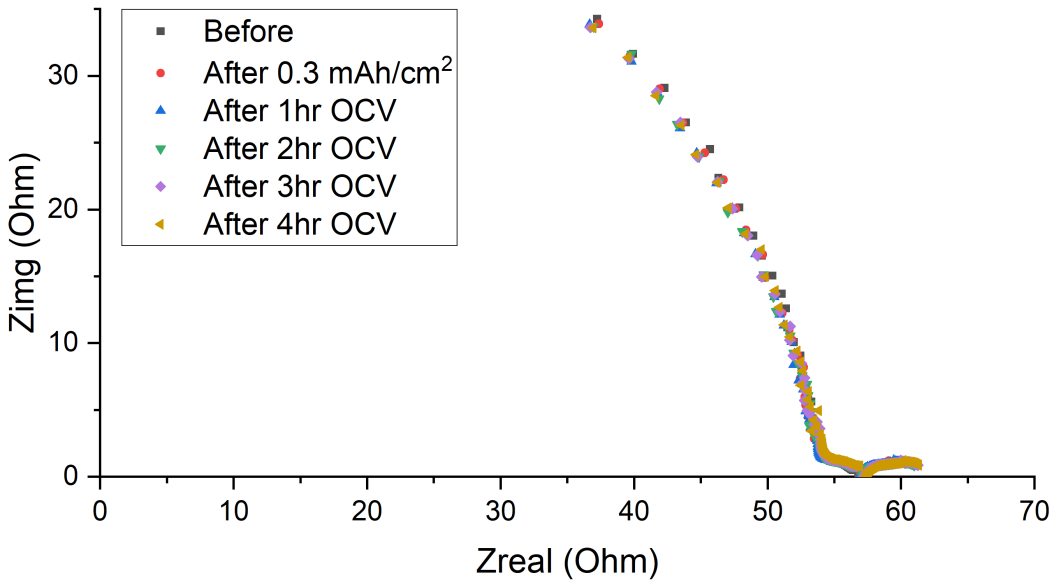

Figure S10. EIS of Li symmetric cell. Nyquist plot of a Li symmetric cell (Li/LPSCl/Li) after discharging a capacity of 0.3 mAh/cm^2 at 1.0 mA/cm^2. EIS was performed every hour during the OCV rest to track the change in impedance with respect to the Li metal counter electrode.

Table S2: Carbon current-interrupt measurements EIS

Cycle Step	0.01 mA/cm^2		0.1 mA/cm^2		1.0 mA/cm^2	
	Bulk Impedance (Ohm*cm^2)	Interfacial Impedance (Ohm*cm^2)	Bulk Impedance (Ohm*cm^2)	Interfacial Impedance (Ohm*cm^2)	Bulk Impedance (Ohm*cm^2)	Interfacial Impedance (Ohm*cm^2)
Before Cycle	13.500	--	14.000	--	12.200	--
0.5 V	13.913	55.353	14.262	465.536	12.197	878.655
0.5 V OCV	13.500	--	14.000	--	12.200	--
0.3 V	13.166	27.090	14.363	57.818	12.516	489.327
0.3 V OCV	12.834	360.822	14.000	--	12.200	--
0.1 V	13.145	4.574	14.700	8.938	12.332	68.321
0.1 V OCV	12.757	7.720	14.355	432.848	12.200	--
0.01 V	12.774	2.528	14.027	3.982	12.721	189.388
0.01 V OCV	12.203	2.982	14.024	8.672	12.200	--
Plating	12.111	1.812	14.099	2.384	12.624	3.876
Plating OCV	11.916	1.871	13.860	2.818	12.615	22.712

Table S3: Carbon current-interrupt measurements OCV Analysis

Cycle Step	0.01 mA/cm^2		0.1 mA/cm^2		1.0 mA/cm^2	
	Voltage after OCV (V)	Delta Voltage (V)	Voltage after OCV (V)	Delta Voltage (V)	Voltage after OCV (V)	Delta Voltage (V)
Before Cycle	1.713	--	1.70458	--	1.7435	--
0.5 V	1.485	0.985	1.674	1.174	1.723	1.223
0.3 V	0.744	0.444	1.375	1.075	1.729	1.429
0.1 V	0.212	0.112	0.778	0.678	1.576	1.476
0.01 V	0.063	0.053	0.223	0.213	1.354	1.343
Plate	0.002	0.002	0.004	0.004	0.395	0.395

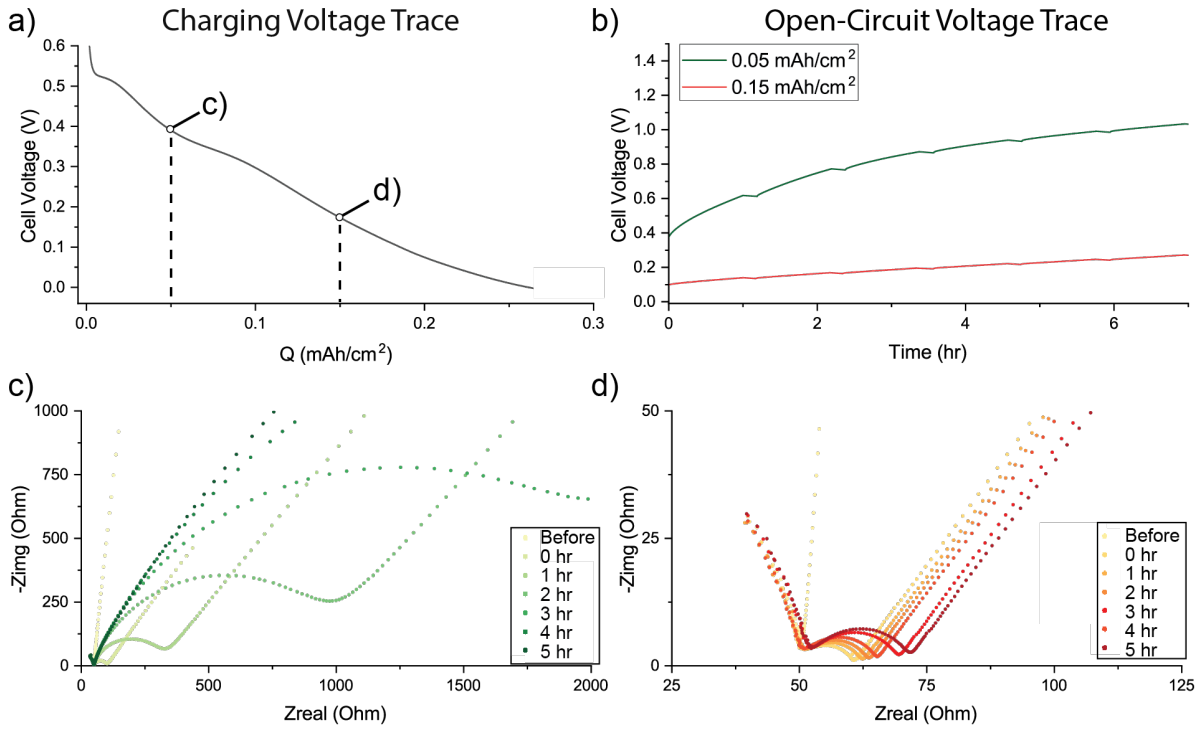

Figure S11. Fixed charging capacity with incremental EIS analysis. (a) Characteristic charging voltage trace of a sample with a carbon interlayer during lithiation at current density of 0.01 mA/cm^2 to a fixed nominal capacity of 0.05 and 0.15 mAh/cm^2. (b) Resulting OCV traces after charging to different capacities. Nyquist plots from EIS performed before charging, immediately after charging, and at one-hour increments for a total of five hours during OCV rest after charging to a capacity of (c) 0.05 mAh/cm^2 and (d) 0.15 mAh/cm^2.

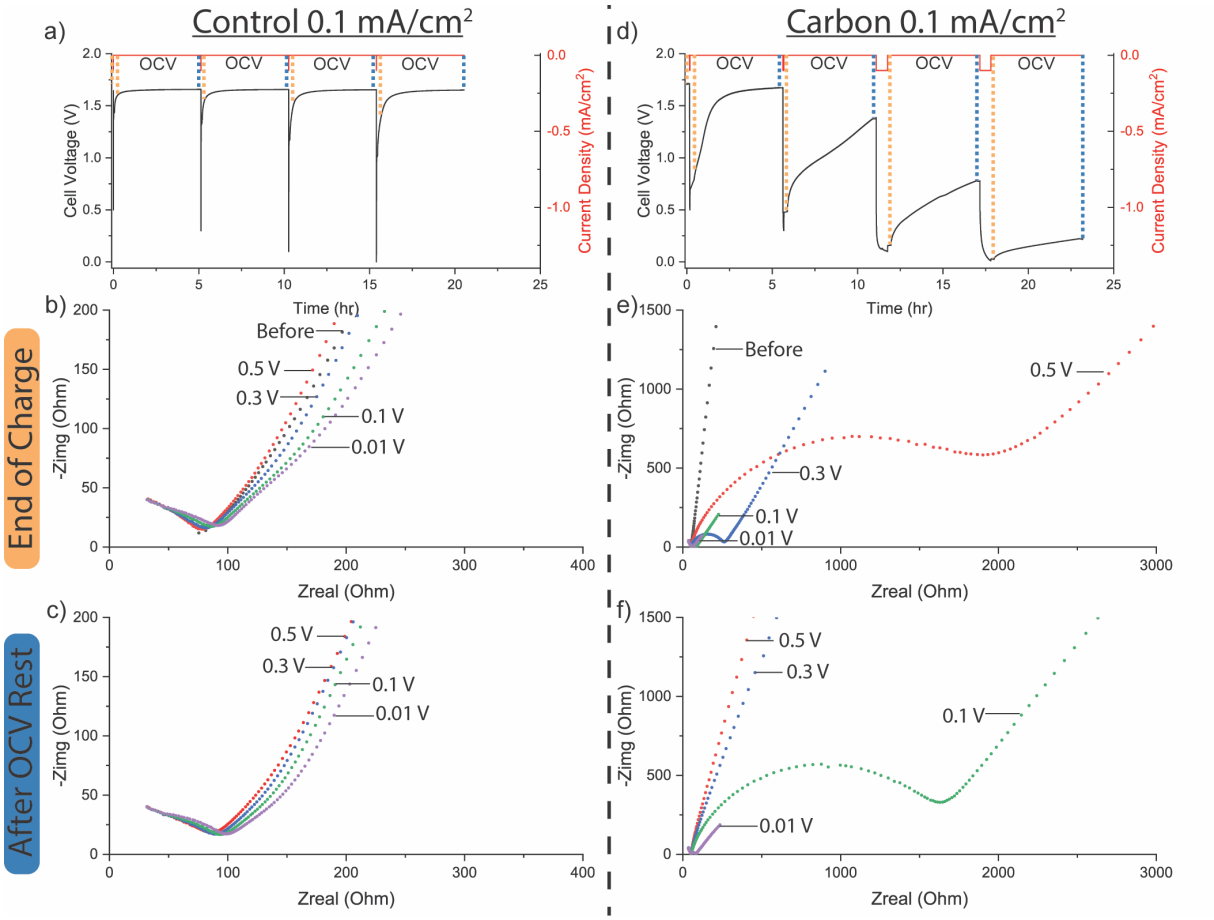

Figure S12. Current-interrupt and EIS measurements of control and carbon interlayer samples at a current density of 0.1 mA/cm². (a) Voltage trace during current-interrupt measurements for a control sample. EIS analysis was performed (b) after the end of each charge step and (c) after the end of each corresponding OCV rest period. (d) Voltage trace during current-interrupt measurements for a carbon interlayer sample. EIS analysis was performed (e) after the end of each charge step and (f) after the end of each corresponding OCV rest period. Note the larger axis scales compared to panels b) and e).

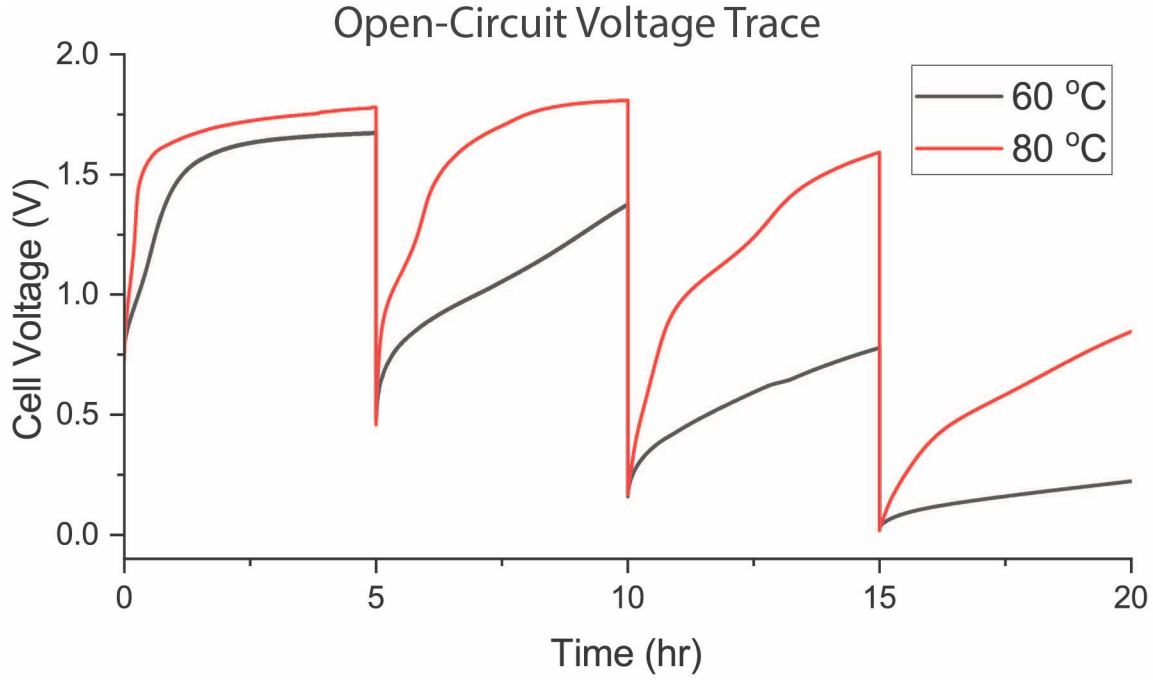

Figure S13. OCV voltage traces during current-interrupt measurements performed at temperatures of 60 °C and 80 °C. Current-interrupt measurements of carbon interlayer electrodes were performed at a current density of 0.1 mA/cm^2, using a voltage cutoff of 0.5, 0.3, 0.1, and 0.01 V. The cell temperature was maintained at 60 °C during charging to minimize differences in the intercalation and plating behavior. The subsequent OCV trace after lithiation to each voltage cutoff during current-interrupt measurements is shown for 60 and 80 °C OCV temperatures.

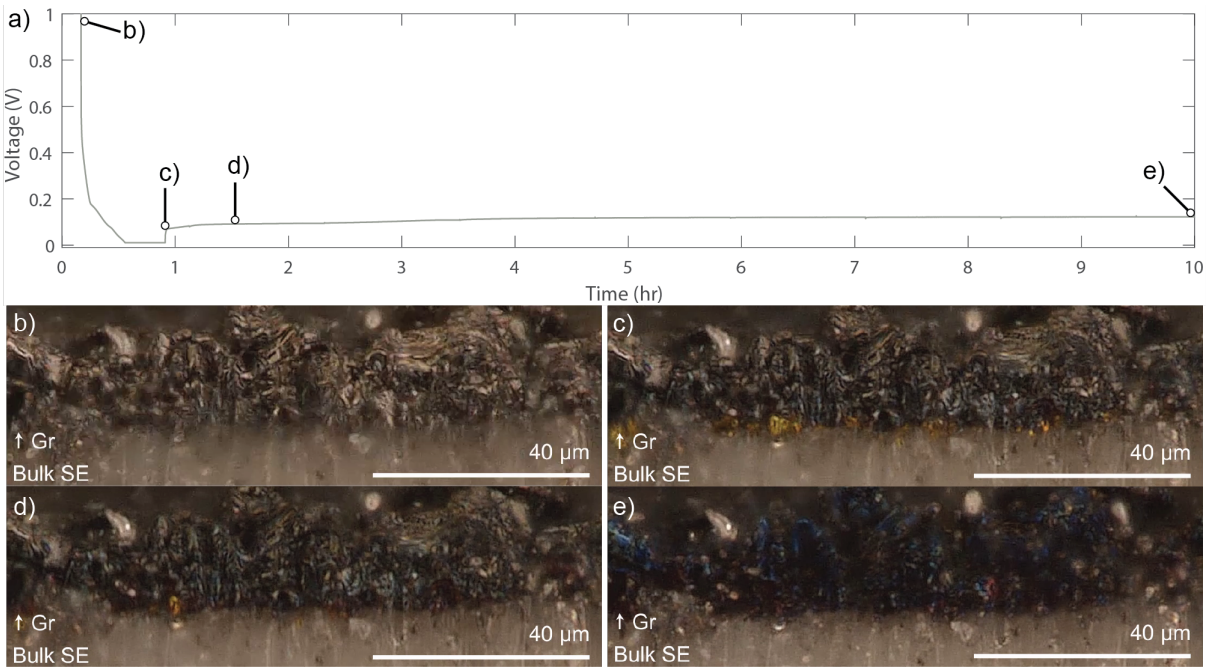

Figure S14. Operando Video Microscopy at high current density. (a) Visualization cell of Gr/LPSCl/Li cell at constant current density of 1 mA/cm^2 to a cutoff voltage of 10 mV followed by a prolonged OCV rest to capture the Li gradient relaxation. A constant-current constant-voltage protocol (CCCV) was used to allow for sufficient capacity passed for visualization of the transition to gold in the graphite particle. Optical images of the cross-section are shown (b) before cycling, (c) after lithiation, (d) after 30-minuteOCV, and (e) after 9-hour OCV.

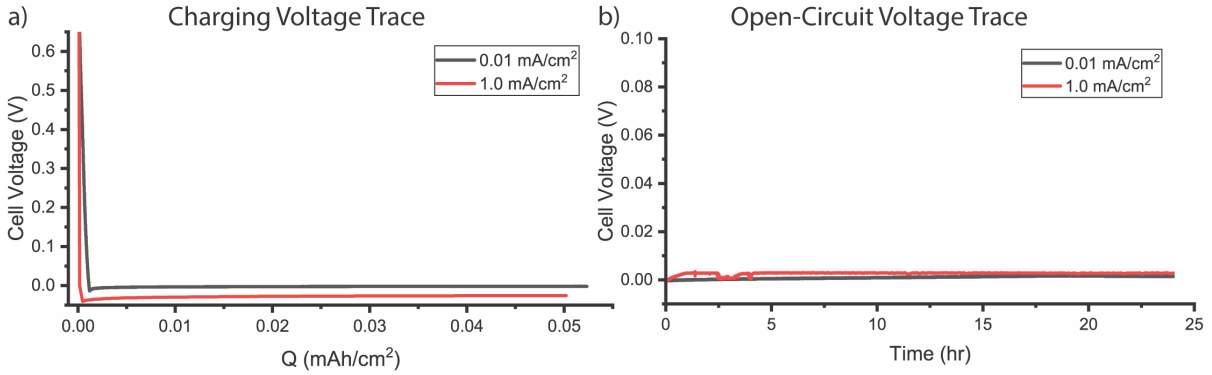

Figure S15. OCV behavior of control samples. (a) Charging voltage trace without a carbon interlayer at current density of 0.01 and 1.0 mA/cm^2 for a plated lithium capacity of 0.05 mAh/cm^2. b) Resulting 24-hour OCV trace of each cell charged at 0.01 and 1.0 mA/cm^2.

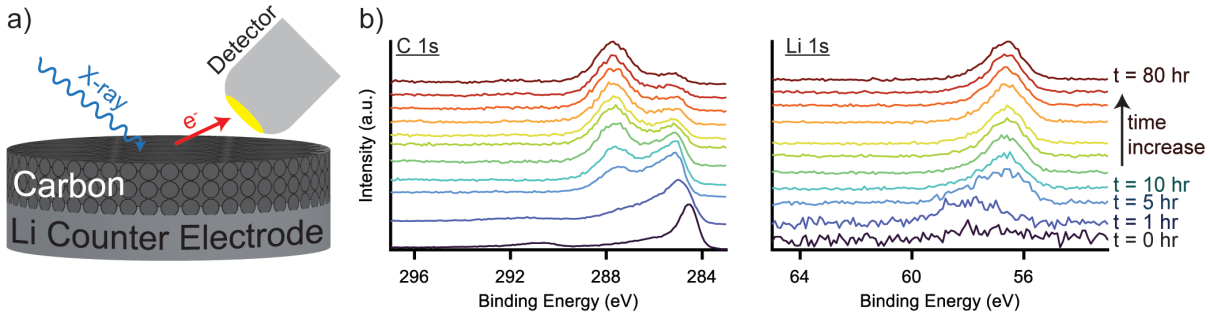

Figure S16. *In-situ* XPS to track solid-state diffusion. (a) Schematic of carbon interlayer in direct contact with metallic Li. (b) XPS Carbon 1s and Lithium 1s core scans performed at 60 °C on the carbon surface that was not in direct contact with the Li. To track gradual lithiation of the carbon interlayer through solid state diffusion, scans were performed at 0, 1, 5, 10, 20, 30, 40, 50, 60, 70, and 80 hours after joining the carbon and Li metal.